

Article

Microwave-Assisted Synthesis of a MK2 Inhibitor by Suzuki-Miyaura Coupling for Study in Werner Syndrome Cells

Mark C. Bagley ^{1,*}, Mohammed Baashen ¹, Irina Chuckowree ¹, Jessica E. Dwyer ¹, David Kipling ² and Terence Davis ²

¹ Department of Chemistry, School of Life Sciences, University of Sussex, Falmer, Brighton, East Sussex, BN1 9QJ, UK; E-Mails: baashen2000@hotmail.com (M.B.); I.Chuckowree@sussex.ac.uk (I.C.); J.E.Dwyer@sussex.ac.uk (J.E.D.)

² Institute of Cancer and Genetics, Cardiff University School of Medicine, Heath Park, Cardiff, CF14 4XN, UK; E-Mails: KiplingD@cardiff.ac.uk (D.K.); davist2@cardiff.ac.uk (T.D.)

* Author to whom correspondence should be addressed; E-Mail: m.c.bagley@sussex.ac.uk; Tel.: +44-1273-873-170.

Academic Editor: Jean Jacques Vanden Eynde

Received: 2 April 2015 / Accepted: 1 June 2015 / Published: 3 June 2015

Abstract: Microwave-assisted Suzuki-Miyaura cross-coupling reactions have been employed towards the synthesis of three different MAPKAPK2 (MK2) inhibitors to study accelerated aging in Werner syndrome (WS) cells, including the cross-coupling of a 2-chloroquinoline with a 3-pyridinylboronic acid, the coupling of an aryl bromide with an indolylboronic acid and the reaction of a 3-amino-4-bromopyrazole with 4-carbamoylphenylboronic acid. In all of these processes, the Suzuki-Miyaura reaction was fast and relatively efficient using a palladium catalyst under microwave irradiation. The process was incorporated into a rapid 3-step microwave-assisted method for the synthesis of a MK2 inhibitor involving 3-aminopyrazole formation, pyrazole C-4 bromination using *N*-bromosuccinimide (NBS), and Suzuki-Miyaura cross-coupling of the pyrazolyl bromide with 4-carbamoylphenylboronic acid to give the target 4-arylpyrazole in 35% overall yield, suitable for study in WS cells.

Keywords: Suzuki-Miyaura; cross-coupling; MK2 inhibitor; Werner syndrome; cell aging; pyrazoles; heterocycles; microwave-assisted synthesis; boronic acid

1. Introduction

Werner syndrome (WS) is an example of a monogenic segmental progeroid syndrome—a rare human autosomal recessive genetic instability syndrome that mimics many, but not all, of the polygenic features of physiological aging [1,2]. It was first characterized by Dr. Otto Werner [3] and its modern diagnosis often relies upon knowledge of previous family incidence and/or presentation with a series of clinical symptoms, including juvenile bilateral cataracts, scleroderma-like skin and premature graying of the hair [4]. Patients manifest a characteristic premature aging phenotype in their twenties or thirties and exhibit an increased predisposition to a number of pro-inflammatory age-related diseases [1], including type II diabetes mellitus, osteoporosis, and atherosclerosis, with premature death occurring typically from cancer or cardiovascular disease. Patients typically have high levels of inflammatory cytokines and intercellular adhesion molecule-1 (ICAM-1) and the same phenomenon can be observed in cell-based studies, with WS fibroblasts showing pronounced activation of inflammatory signaling pathways [5–7]. As a result, WS is often classified as an example of “inflamm-aging” [5,7] to highlight its association with, and patient pre-disposition to, age-related inflammatory disease pathologies [8]. The genetic basis of WS is known, with WS resulting from mutations in the RecQ3 DNA helicase-encoding gene *WRN* that give rise to a pathology attributed for the most part to the key role of RecQ3 in cellular responses to specific types of DNA damage. Lack of RecQ3 leads to frequent DNA replication fork stalling and subsequently genomic instability [9] and WS is classified as a chromosome instability syndrome [10]. The replication fork stalling and an increased pro-oxidant state [11] could provide the trigger for replication stress in WS leading to a decreased ability for WS cells to undergo division [5]. This is supported by the observation that young WS cells show a much reduced division capability compared to cells from normal individuals and resemble fibroblasts that have undergone stress-induced premature senescence [12], which is known from many different stimuli to be transduced by the mitogen activated protein kinase (MAPK) p38 [13–15]. This implicates the involvement of p38 signaling in the premature cell cycle arrest in WS and the short replicative life span observed in WS cell cultures. This in turn implicates a reduced ability of WS cells to divide as an underlying cause of accelerated aging in WS [2].

1.1. Studies of P38 Inhibitors in WS Cells

The role of stress signaling in Werner syndrome cells has been investigated using a range of small molecule inhibitors (Figure 1) of p38 MAPK [16], including SB203580 [12,17,18], VX-745 [19–21], RO3201195 [22,23], UR-13756 [24], and BIRB 796 [25], to study the link between replicative senescence *in vitro* and *in vivo* pathophysiology. WS fibroblasts treated with a p38 inhibitor display an unexpected reversal of the accelerated aging phenotype [12] and, as such, this may provide a suitable model for future therapeutic interventions designed to combat the aging process itself [12,26].

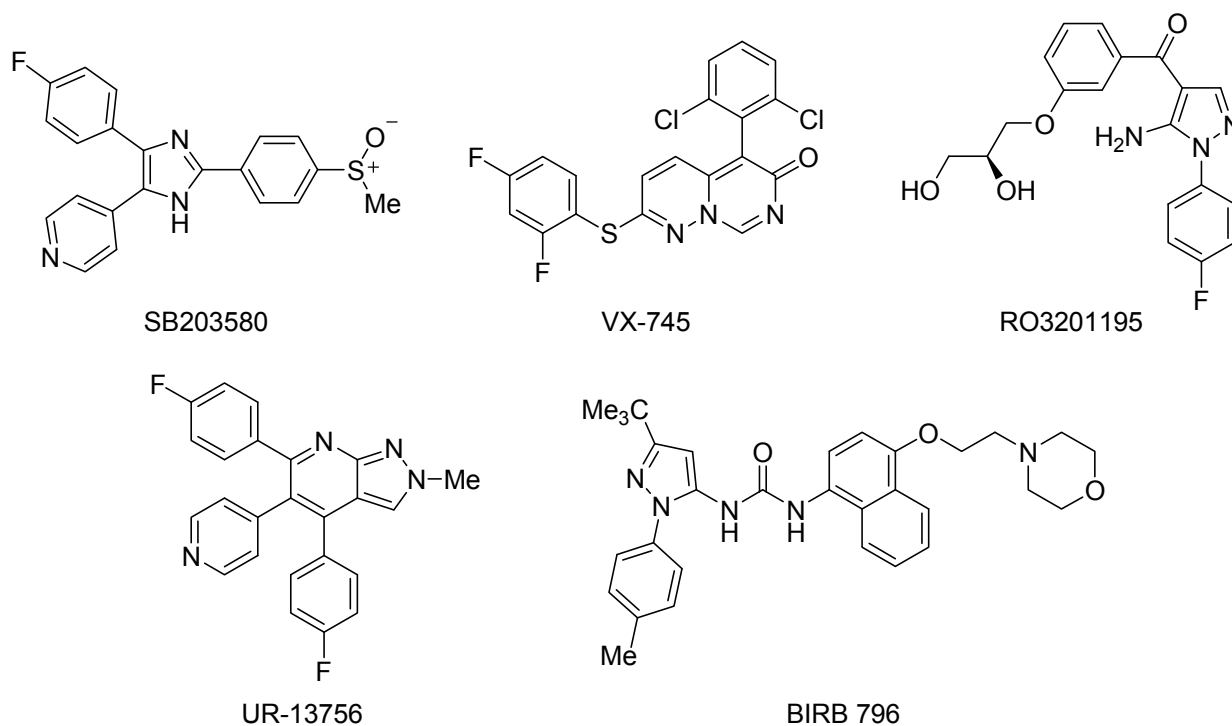


Figure 1. Inhibitors of p38 MAPK examined in WS cells.

1.2. Synthesis and Properties of MK2 Inhibitors

Although progress in the clinical development of successful p38 inhibitors for *in vivo* use is currently a considerable challenge [27], probably frustrated by toxicity issues, it may be possible to elicit a similar biological response by targeting the downstream kinase MAPKAPK2 (MK2) [16,28], which may itself be involved in the phenotypic characteristics seen in WS, including enlarged cellular morphology and prominent F-actin stress fibres [12]. MK2 activity up-regulates the expression of inflammatory pathways [29] and recent data suggest that MK2 acts as a checkpoint kinase that can lead to cell cycle arrest [30]. Furthermore MK2 knock-out mice exhibit normal, healthy phenotypes and are inflammation resistant [31], whereas p38 knock-out mice are lethal [32]. This could indicate that chemical inhibition of MK2 may be less problematic than inhibition of p38, whilst providing similar *in vivo* efficacy.

As a consequence of these observations, there has been considerable recent activity in drug discovery programs to develop small molecule inhibitors of MK2 [33]. A number of different chemotypes have been investigated [34], including a series of pyrrolopyridines **1** [35], pyrazinoindolone **2** [36], the benzo[4,5]thieno[3,2-*e*][1,4]diazepinone PF-3644022 [37] and recently tricyclic lactams **3** as a non-ATP-competitive inhibitor scaffold [38], yet issues of selectivity, potency and/or toxicity remain [34,39]. Many, but not all, of these approaches used Suzuki-Miyaura reactions to introduce diversity to an advanced intermediate for scaffold optimization (Figure 2). Since its initial discovery as a Pd-catalyzed stereospecific cross-coupling reaction of 1-alkenylboranes [40], the Suzuki-Miyaura reaction has become one of the most efficient methods for C–C bond formation, in particular for aryl-aryl coupling [41]. It offers many advantages over other methods, in that it is largely unaffected by the presence of water, produces non-toxic inorganic by-products that are easily removed, tolerates

a broad range of functional groups and proceeds generally with regio- and stereocontrol [42]. In a recent analysis of reactions used in the pursuit of drug candidates taken from a 2008 data set [43], biaryl linkages were present in 40% of the compounds that were analyzed and the Suzuki-Miyaura reaction occurred in over 4% of all reactions and in 40% of all C–C bond forming reactions. Given the amenability of transition-metal mediated processes to be accelerated under microwave dielectric heating [44], and thus readily automated to probe SAR, it is perhaps not surprising to observe so many uses of this reaction in the development of MK2 inhibitors [28] and such a high occurrence of this reaction in drug discovery programs in general [44].

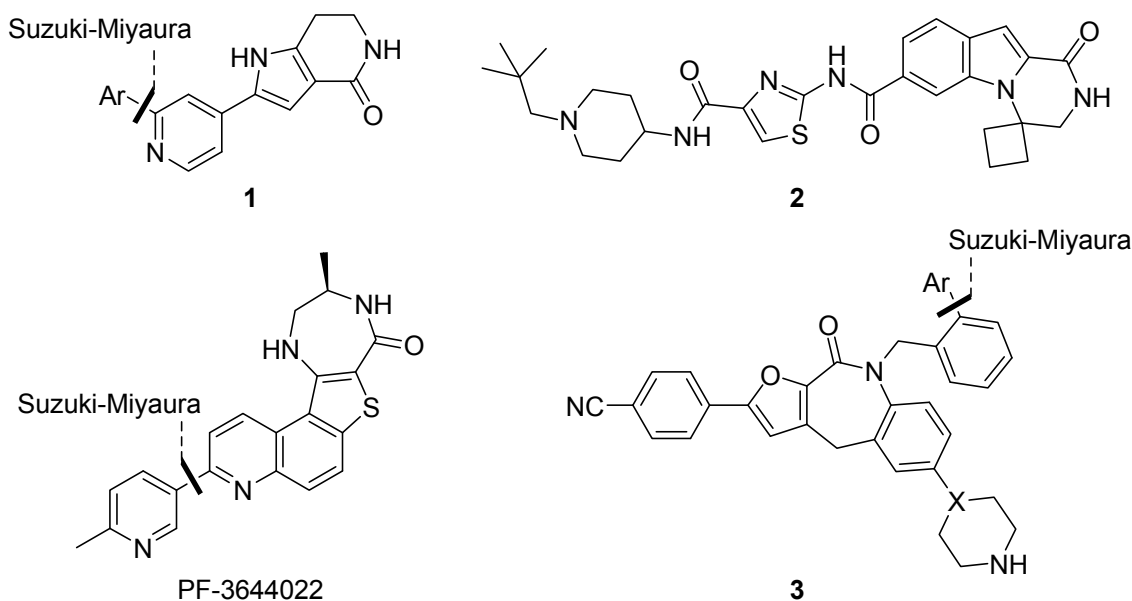


Figure 2. Examples of MK2 inhibitors from different drug discovery programs, showing the use of Suzuki-Miyaura aryl-aryl coupling for late-stage scaffold optimization.

Given the success of a p38 inhibitor in rescuing accelerated aging in WS cells, we carried out studies on a number of MK2 inhibitors (Figure 3) to establish their effect on cell aging phenotypes using fibroblasts from human WS [28,45,46]. Of these inhibitors, butyramide **4** was reported to act by blocking p38-MK2 docking, thus preventing the activation of MK2 by phospho-p38 [47] but in WS cells caused a stressed morphology and permanent cell cycle arrest [46] by a pathway that appeared not to involve MK2 inhibition [46]. A benzopyranopyridine inhibitor **5** [48] gave a similar cellular response at a concentration that inhibited MK2, but this was thought to be due to non-specific toxicity issues [46]. However, when primary WS fibroblasts were treated with a tetrahydropyrrolo[3,2-*c*]pyridin-4-one inhibitor **6**, the stressed cellular morphology and shortened replicative lifespan were both corrected, although the extension in life span was much smaller than the one seen upon treatment with SB203580 [45]. Given this promising indication, and the wide range of MK2 inhibitors investigated in other cellular models, a rapid route to another MK2 inhibitory chemotype was urgently required to provide added confirmation of the above findings.

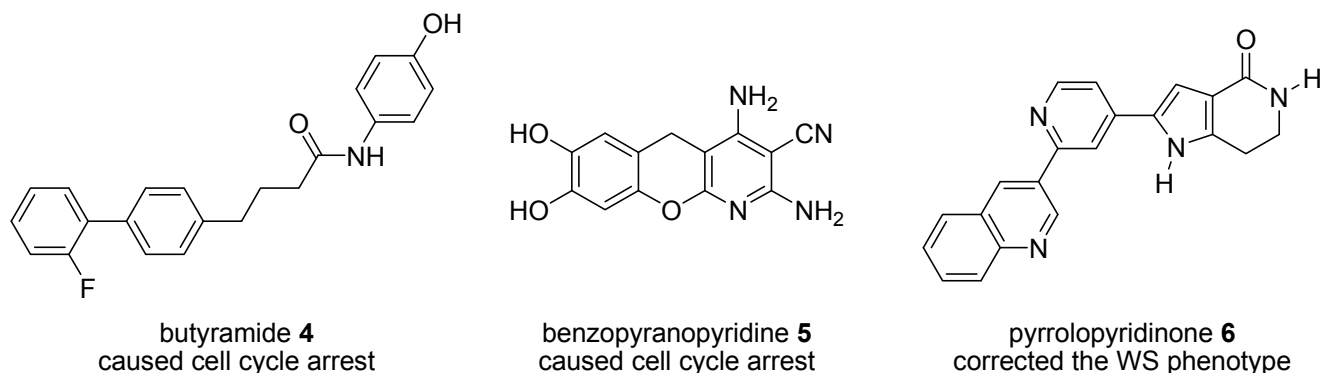


Figure 3. MK2 inhibitor chemotypes and their effect on WS cells.

2. Results and Discussion

Our first approach aimed to take advantage of the Suzuki-Miyaura coupling in a rapid route to the Pfizer MK2 inhibitor PF-3644022 [37,49,50]. Although this compound exhibits single digit nanomolar potency against MK2 (IC_{50} 5 nM), cellular activity below 500 nM (U937 TNF α release IC_{50} 150 nM) [50], good selectivity across 200 human kinases and projected human pharmacokinetics sufficient for oral dosing, it was found to lead to acute hepatotoxicity in dogs, probably by disrupting hepatobiliary transporters [39]. Nevertheless, for study in WS cells, its activity and selectivity profile made it a compelling target, with preliminary data using this inhibitor showing extension of cellular replicative capacity in WS fibroblasts and correction of the stressed morphology (Figure 4), a result similar in magnitude to that seen using the tetrahydropyrrolo[3,2-*c*]pyridin-4-one inhibitor **6** [45].

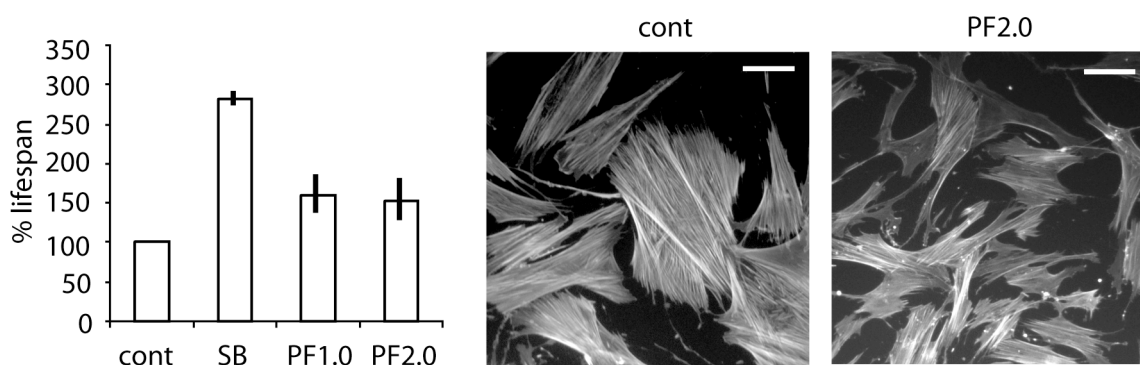


Figure 4. Increased replicative lifespan (\pm SD; $n = 3$) and improvement cellular morphology in WS cells using PF-3644022. Cont = control, SB = SB203580 at 2.5 μ M, PF1.0 and PF2.0 = PF-3644022 at 1.0 and 2.0 μ M respectively. White bar = 100 μ m (for methods see experimental section).

The development of this inhibitor utilized a late-stage Suzuki-Miyaura coupling to introduce diversity at C-7 of a thieno[3,2-*f*]quinoline ring (see Figure 2) [49], following initial identification of promising SAR studies and cellular potency with a benzo[4,5]thieno[3,2-*e*][1,4]diazepin-5(2*H*)-one scaffold [50]. Given that our goal was the introduction of a 6-methyl-3-pyridyl substituent at C-7, we set out to incorporate the Suzuki-Miyaura coupling of the pyridinylboronic acid **10a** and 2-chloroquinoline **11** into an early stage of the synthesis (Figure 5). Elaboration of the target inhibitor should then

proceed in a similar fashion to Anderson's route [49]: one-step formation of aminocyanquinoline **8a** from nitroquinoline **9a**, followed by synthesis of aminobenzothiophene **7** by diazotization and subsequent reaction with methyl thioglycolate before the introduction of the diazepinone ring.

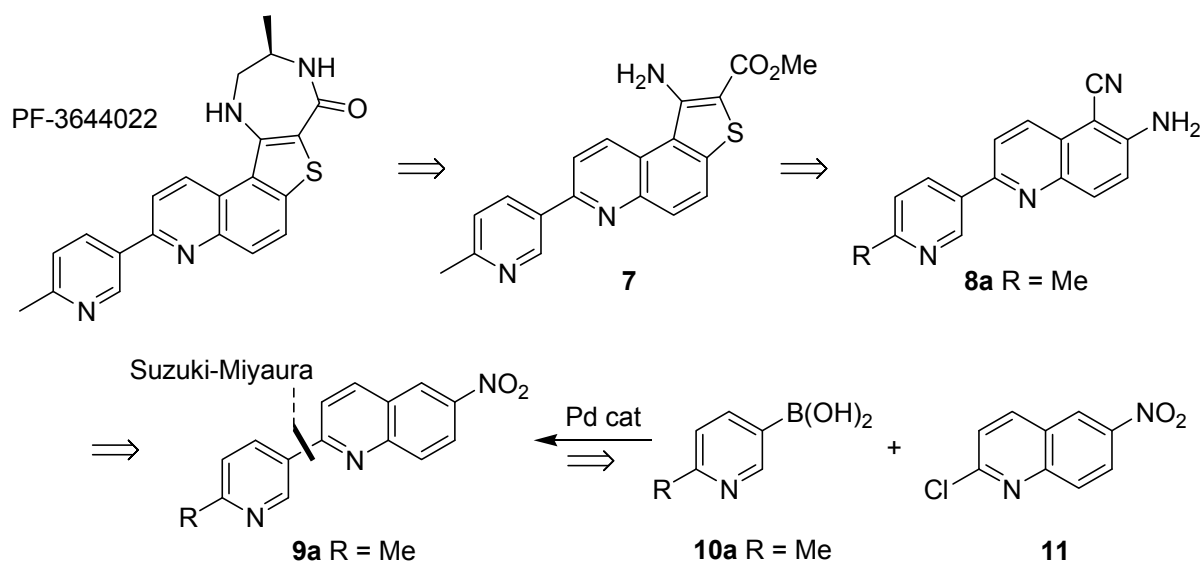


Figure 5. Disconnective approach to the synthesis of PF-3644022, utilizing an early-stage Suzuki-Miyaura cross-coupling reaction.

2.1. Early-Stage Suzuki-Miyaura Cross-Coupling Reactions for the Synthesis of PF-3644022

Starting with a known route to **11** [51], 3,4-dihydroquinolin-2(1H)-one (**12**) was nitrated using $\text{HNO}_3/\text{H}_2\text{SO}_4$ and then treated with phosphorus oxychloride in DMF in the presence of DDQ as oxidant to give 2-chloro-6-nitroquinoline (**11**) in 90% isolated yield over the two steps (Figure 5). Suzuki-Miyaura cross-coupling with 6-methyl-3-pyridinylboronic acid (**10a**) using Na_2CO_3 base and $\text{PdCl}_2(\text{PPh}_3)_2$ as catalyst in $\text{MeCN}-\text{H}_2\text{O}$ at $140\text{ }^\circ\text{C}$ under microwave irradiation gave the cross-coupled product **9a** in reasonable yield. However, use of the Yamazaki method for the synthesis of *ortho*-aminoaroylnitriles [52], namely treating nitroquinoline **9a** with ethyl cyanoacetate and KOH in DMF at room temperature for up to 72 h, followed by hydrolysis using 5% NaOH (aq) at reflux for 3 h, in accordance with Anderson's approach, gave only a trace of the 6-amino-5-cyanoquinoline **8a**. Given the wide range of nitroquinolines compatible with this chemistry in Yamazaki's original report [52], and its previous use in a route to PF-3644022 by Anderson [49], this was unexpected. To probe whether the acidity of the pyridine 6-methyl group had been responsible for this observation, the Suzuki-Miyaura cross-coupling reaction was repeated using 3-pyridinylboronic acid (**10b**), to give the 2-pyridylquinoline **9b** in 62% isolated yield (Figure 6). When this substrate was investigated in the Yamazaki cyanation reaction under identical conditions it behaved in a very similar fashion and only a trace of the cyanoquinoline product **8b** was observed by ^1H NMR spectroscopic analysis of a complex mixture. Efforts to introduce the Yamazaki cyanation at an earlier stage in the process were similarly unsuccessful. Dihydroquinolone **13** was inert to treatment with ethyl cyanoacetate and KOH in DMF, either at room temperature for 24 h followed by treatment with aqueous base or under more forcing conditions, when heated to $50\text{ }^\circ\text{C}$ for 64 h. In both cases only unreacted starting material **13** was

obtained. Alternatively, when chloroquinoline **11** was reacted with ethyl cyanoacetate in the presence of base at RT for 64 h (Figure 6) a complex mixture of products was obtained, rather than cyanoquinoline **8c**. It was apparent that either the lactam ring or an electrophilic chloroquinoline function interfered unfavorably with this cyanation reaction. For comparison, Yamazaki cyanation of 6-nitroquinoline (**14**) under identical conditions gave the expected product, 6-amino-5-cyanoquinoline (**15**) in good yield (72%) after basic hydrolysis. Thus it was concluded that an early-stage Suzuki-Miyaura cross-coupling strategy was efficient for biaryl C-C bond formation but the 2-pyridylquinoline products, as well as other quinoline-containing precursors, were incompatible with Yamazaki's aminoaroylnitrile synthesis and so could not be used for the rapid synthesis of the MK2 inhibitor, PF-3644022.

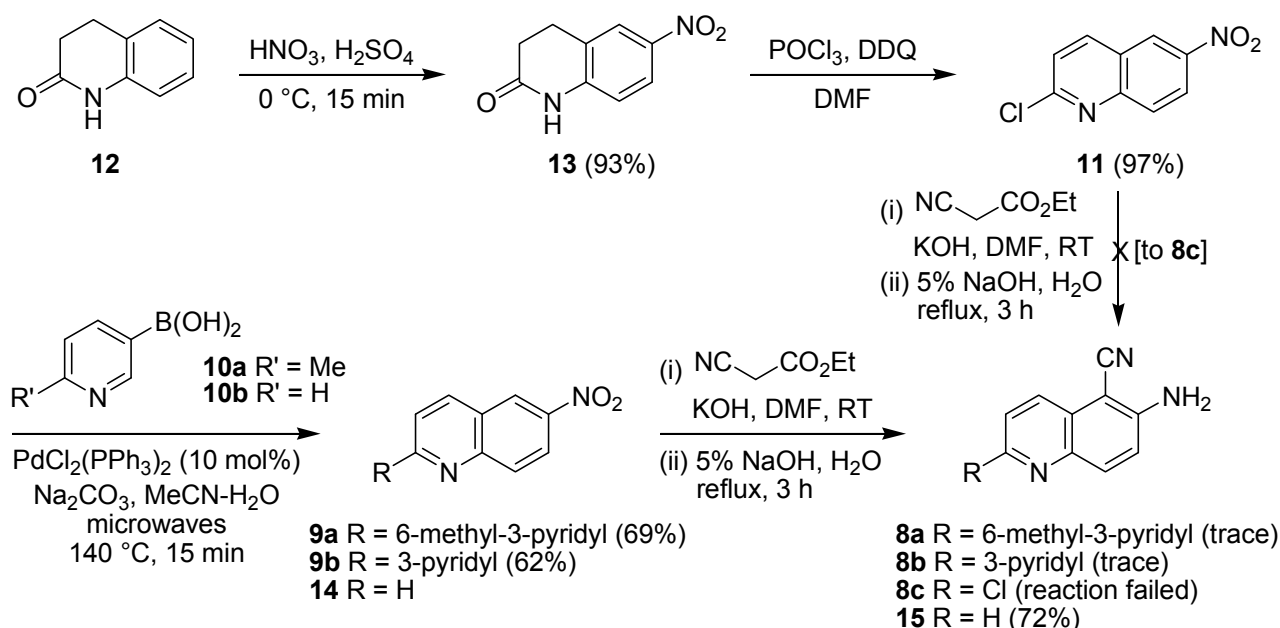


Figure 6. Synthesis of chloroquinoline **11** and subsequent Suzuki-Miyaura cross-coupling.

2.2. Suzuki-Miyaura Cross-Coupling Reactions for the Synthesis of (Indolyl)phenylpyrazole MK2 Inhibitor **18**

Given the success of pyrrolopyridinone **6** in correcting the WS phenotype, we next turned to the scaffold hopping strategy of Velcicky *et al.* [53] for rapid access to a MK2 inhibitor for study in WS cells. Velcicky found that replacing the pyrrolopyrimidinone pharmacophore **16**, which overlays well with pyrrolopyridinone **6**, with a series of benzamide derivatives **17** led to the development of a 3-aminopyrazole **18** that inhibited intracellular phosphorylation of HSP27, as well as LPS-induced TNF α release in cells (Figure 7) [53]. The synthesis of this inhibitor employed two successive Suzuki-Miyaura cross-coupling reactions to establish the biaryl bonds. Given our recent report on the regiocontrolled synthesis of 3-aminopyrazoles [54], this was a compelling scaffold to study.

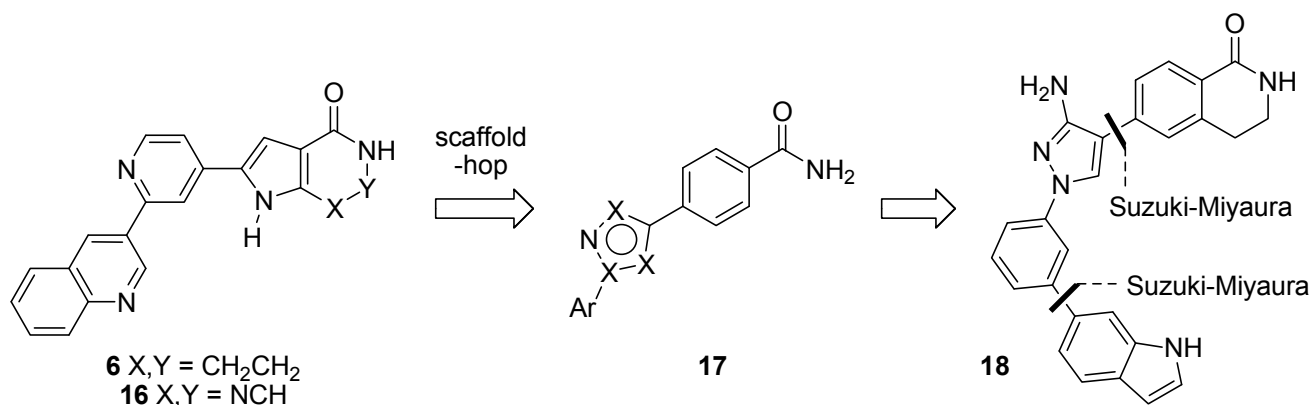


Figure 7. Scaffold-hopping strategy of Velcicky *et al.* [53], showing the use of Suzuki-Miyaura aryl-aryl coupling for scaffold optimization.

The hydrochloride salt of 3-bromophenylhydrazine (**19**) was reacted with 3-methoxyacrylonitrile (**20**) (2 equiv.) in the presence of a large excess of sodium ethoxide in ethanol at reflux for 20 h (Figure 8) to give 3-aminopyrazole **21** in excellent yield (90%), or more rapidly under microwave irradiation at 150 °C for 1 h in a sealed tube to give the same product in comparable yield (89%) [54]. Under the strongly basic conditions, no 5-aminopyrazole regioisomers were isolated or observed. Efforts to improve the microwave-assisted procedure, by switching to *tert*-butyl alcohol in the presence of *tert*-butoxide as base and irradiating at 150 °C for 2 h caused a significant reduction in yield (68%) and so the overnight conductive heating method was adopted as the procedure of choice as it could be readily carried out on gram scale. Suzuki-Miyaura cross-coupling of the arylbromide **21** with 6-indolylboronic acid **22** under microwave irradiation at 150 °C for 2 h in DMF in the presence of cesium carbonate and tetrakis(triphenylphosphine)palladium(0) (10 mol%) gave the coupled product **23** in 84% isolated yield. Unfortunately, bromination at C-4 of aminopyrazole **23** using NBS failed to provide 4-bromopyrazole **24** and instead gave a complex mixture of products, presumably due to competing bromination of the indolyl ring. It was possible to install the C-4 bromo group prior to Suzuki-Miyaura coupling by treating the *N*-(bromophenyl)pyrazole **21** with NBS in THF at RT for 16 h to give dibromide **25** in 83% yield after purification by column chromatography. However, Suzuki-Miyaura cross-coupling of dibromide **25** with the 6-indolylboronic acid **22** under similar conditions did not provide the 4-bromopyrazole **24** and instead gave a complex mixture of products and could not differentiate between the two reactive sites. Although potentially this could be resolved through the use of different halogen moieties, given the difficulties or the need to use protecting group chemistries for the synthesis of the indole-containing inhibitor, we switched to a simpler pyrazole target, benzamide **26**, reported to possess reasonable potency (IC₅₀ 2.0 μM), as a more accessible inhibitor for evaluation in WS cells.

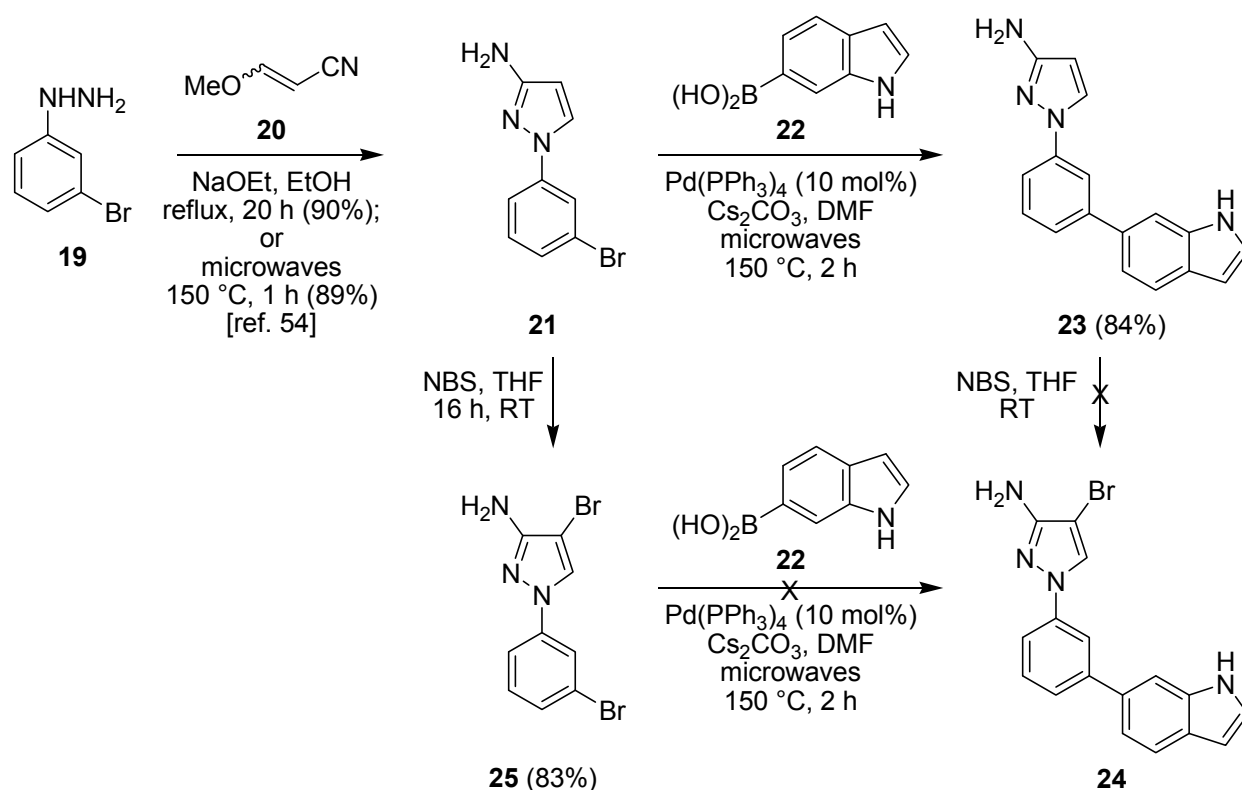


Figure 8. Suzuki-Miyaura cross-coupling for the synthesis of 6-indolyl scaffolds.

2.3. Suzuki-Miyaura Cross-Coupling Reactions for the Synthesis of Aminopyrazole MK2 Inhibitor **26**

Adopting a similar route, the hydrochloride salt of 4-methoxyphenylhydrazine (**27**) was reacted with 3-methoxyacrylonitrile (**20**) (2 equiv.) under basic conditions using sodium ethoxide in ethanol under microwave irradiation at 150 °C for 2 h to give 3-aminopyrazole **28** as the only observed regioisomer in 85% yield (Figure 9). Bromination using NBS in THF under microwave irradiation at 150 °C for 2 h gave the C-4 brominated pyrazole **29** in 77% yield. This rapid microwave-assisted procedure was preferred over a method under ambient conditions, which required stirring with NBS in THF for 16 h but did give bromide **29** in slightly improved yield (82%). Suzuki-Miyaura coupling of the pyrazolylbromide **29** with 4-carbamoylphenylboronic acid (**30**) in *i*PrOH–H₂O in the presence of potassium carbonate and bis(triphenylphosphine)palladium(II) chloride (10 mol%) under microwave irradiation at 150 °C for 2 h using similar conditions to Velcicky *et al.* [53] gave the coupled product **26** in 54% yield after purification by column chromatography. This route to pyrazole **26** utilized three microwave-assisted steps, each of 2 h duration, starting from commercially-available materials and provided the target MK2 inhibitor in 35% overall yield, suitable for study in WS cells.

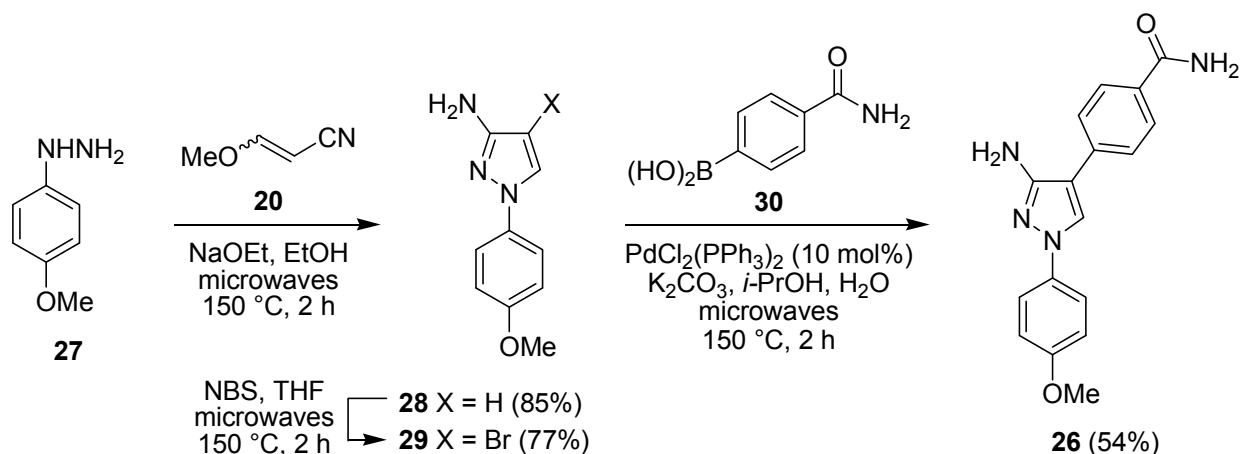


Figure 9. Microwave-assisted synthesis of the MK2 inhibitor **26** using a Suzuki-Miyaura cross-coupling.

2.4. Biological Evaluation of Aminopyrazole MK2 Inhibitor **26** in WS Cells

When WS fibroblasts were grown in the presence of inhibitor **26** at 25 μM a small lifespan extension was noted, although it was difficult to ascertain if this was significant, especially as little inhibition of MK2 activity was seen at this concentration [28]. Treatment with inhibitor **26** did, however, show improvement in the cellular morphology of the WS cells at 25 μM and 50 μM . These results were encouraging for the further development of MK2 inhibitors in this and other inflammatory therapeutic areas.

2.5. The Role of MK2 in the WS Cell Phenotype and Its Modulation Using Chemical Inhibitors

Effects of MK2 inhibitors on the growth and morphology of WS cells have been ambiguous: inhibitors **4** and **5** resulted in growth inhibition that was not related to MK2 inhibition [46]; inhibitor **6** increased cellular replicative capacity at a concentration that maximally inhibited MK2 [45]; inhibitor **26** showed a small increase in replicative capacity and alleviated the stressed morphology [28]; and finally, PF-3644022 had an effect similar in magnitude to inhibitor **6** at a dose that fully inhibited MK2 (this work). Thus, three MK2 inhibitors with very different chemotypes gave similar results for WS fibroblasts on all cellular parameters tested. These data suggest a role for p38-activated MK2 in replicative senescence in WS fibroblasts, although this role appears to be much reduced compared to that of p38, as the p38 inhibitor SB203580 has much larger effects on the replicative capacity of WS fibroblasts [12]. Possible reasons for the reduced effects of MK2 inhibitors on replicative capacity are that MK2 may be only one of the downstream effectors of p38 responsible for cellular growth arrest [55], or that MK2 inhibitors have a narrow therapeutic window and become toxic to cell growth at levels close to the maximally effective dose [34]. This latter is seen with both PF-3644022 that is effective at 2.0 μM but becomes toxic to cell growth at levels of 5.0 μM and above (unpublished data), and with inhibitor **6** that is maximally effective at 5.0 μM but toxic at 10.0 μM [45]. These data also suggest that MK2 inhibitors may not be as useful therapeutically as p38 inhibitors if the accelerated cell aging seen in WS does underlie the accelerated whole body aging, as suggested [2], but may prove useful in the alleviation of the associated inflammatory conditions that are thought to be MK2 dependent [29].

As inflammatory conditions that may be due to MK2 activation are an increasing issue during the normal human aging process [56], such inhibitors may be of wider therapeutic benefit in the general population. This then provides a good rationale for the continued efforts to find suitable MK2 inhibitors for *in vivo* use.

3. Experimental Section

3.1. Synthetic Materials and Methods

Commercially available reagents were used without further purification; solvents were dried by standard procedures. Light petroleum refers to the fraction with bp 40–60 °C and ether (Et₂O) refers to diethyl ether. Column chromatography was carried out using Merck Kieselgel 60 H silica or Matrex silica 60. Analytical thin layer chromatography was carried out using aluminium-backed plates coated with Merck Kieselgel 60 GF₂₅₄ that were visualised under UV light (at 254 and/or 360 nm). Microwave irradiation experiments were performed in a sealed Pyrex tube using a self-tunable CEM Discover or CEM Explorer focused monomodal microwave synthesizer at the given temperature using the instrument's in-built IR temperature measuring device, by varying the irradiation power (initial power given in parentheses).

Fully characterized compounds were chromatographically homogeneous. Melting points (mp) were determined on a Kofler hot stage apparatus or Stanford Research Systems Optimelt and are uncorrected. Infra-red (IR) spectra were recorded in the range 4000–600 cm⁻¹ on a Perkin-Elmer 1600 series FTIR spectrometer using an ATR probe or as a KBr disk (KBr) and are reported in cm⁻¹. Nuclear magnetic resonance (NMR) spectra were recorded in CDCl₃ at 25 °C unless stated otherwise using a Varian VNMRS instrument operating at 400 or 500 MHz or a Bruker DPX 400 or 500 Avance instrument operating at 400 or 500 MHz for ¹H spectra and 100 or 126 MHz for ¹³C spectra and were reported in ppm; *J* values were recorded in Hz and multiplicities were expressed by the usual conventions (s = singlet, d = doublet, t = triplet, app = apparent, m = multiplet, br = broad). Mass spectra (MS) were determined with a Fisons VG Platform II Quadrupole instrument using atmospheric pressure chemical ionization (APCI), a Waters Q-TOF Ultima using electrospray positive ionization (ES), a Waters LCT premier XE using atmospheric pressure chemical ionization (APCI), an Agilent 6130 single quadrupole with an APCI/electrospray dual source, a Fisons Instrument VG Autospec using electron ionization (EI) at 70 eV (low resolution) or a ThermoQuest Finnigan LCQ DUO electrospray, unless otherwise stated. Some high-resolution mass spectra were obtained courtesy of the EPSRC Mass Spectrometry Service at Swansea, UK using the ionisation methods specified. *In vacuo* refers to evaporation at reduced pressure using a rotary evaporator and diaphragm pump, followed by the removal of trace volatiles using a vacuum (oil) pump.

3.2. General Synthetic Procedures

General Procedure for Suzuki-Miyaura Cross-Coupling

A solution of 2-chloro-6-nitroquinoline, boronic acid (1.5–1.6 equiv.), aqueous Na₂CO₃ solution (2 equiv.) and PdCl₂(PPh₃)₂ (10 mol%) in MeCN (0.2 M) was irradiated at 140 °C for 15 min in a

pressure-rated glass tube (35 mL) using a CEM Discover microwave synthesizer by moderating the initial power (200 W). After cooling in a flow of compressed air, the solvent was evaporated *in vacuo* and the residue was triturated with water. Purification by flash column chromatography on SiO₂ gave the desired 2-pyridinyl-6-nitroquinoline.

3.3. Synthetic Experimental Procedures

3.3.1. 3,4-Dihydro-6-nitroquinolin-2(1H)-one (**13**)

According to a known literature procedure [51], concentrated sulfuric acid (20 mL) was added to 3,4-dihydro-2-(1H)-quinoline (**12**) (1.00 g, 6.79 mmol) in a 100 mL round-bottom flask. The reaction was placed into an ice-acetone bath (−10 °C approx.) and stirred to dissolve the solid. Nitric acid (69%; 0.50 mL, 11.3 mmol, 1.7 equiv.) was added dropwise and the orange-red solution was stirred at −10 to 0 °C for 30 min. The reaction was quenched by pouring onto a stirred ice-water slush (300 mL). The ice was allowed to melt and the precipitate was collected by vacuum filtration, washed with water and air dried under suction to give a beige-coloured solid (1.21 g, 93%), with identical physical and spectroscopic properties to literature data [51].

3.3.2. 2-Chloro-6-nitroquinoline (**11**)

POCl₃ (1.2 mL, 13.0 mmol) was added dropwise to a stirred solution of **13** (1.00 g, 5.2 mmol) and DDQ (1.30 g, 5.7 mmol) in DMF (20 mL) and the reaction mixture was stirred at RT for 1 h. The reaction mixture was then poured into iced water and the resultant precipitate was collected by vacuum filtration, washed with water and dried in air to give the *title compound* (1.05 g, 97%) as an orange solid, mp 226.8–227.9 °C (lit. [51] mp 235.5–236.5 °C) (Found [ES]: MH⁺, 209.0112. C₉H₆ClN₂O₂ [MH] requires 209.0112); IR (neat) ν_{max}/cm^{-1} 3068 (C-H), 1619 (C=C), 1523 (NO₂), 1485 (C=C), 1337 (NO₂), 1105 (C-N); ¹H-NMR (500 MHz, *d*₆-DMSO) δ_H/ppm 9.13 (1H, d, *J* 2.5, 5-CH), 8.78 (1H, d, *J* 9, 4-CH), 8.52 (1H, dd, *J* 9, 2.5, 7-CH), 8.18 (1H, d, *J* 9, 8-CH), 7.84 (1H, d, *J* 9, 3-CH); ¹³C-NMR (126 MHz, *d*₆-DMSO) δ_C/ppm 153.6 (C), 149.2 (C), 145.3 (C), 141.9 (4-CH), 129.7 (8-CH), 125.9 (C), 125.0 (5-CH), 124.4 (3-CH), 124.1 (7-CH); *m/z* (EI) 208 (M⁺, 100), 162 (48), 150 (49), 127 (81).

3.3.3. 2-(6-Methylpyridin-3-yl)-6-nitroquinoline (**9a**)

Biaryl **9a** was prepared according to general synthetic procedure 3.2.1 using 2-chloro-6-nitroquinoline (**11**) (0.45 g, 2.20 mmol), 6-methyl-3-pyridinylboronic acid (**10a**) (0.44 g, 3.20 mmol), aqueous Na₂CO₃ solution (1.5 M; 3 mL) and PdCl₂(PPh₃)₂ (0.15 g, 0.21 mmol) in MeCN (12 mL). Purification by column chromatography on SiO₂ gel, gradient eluting with CH₂Cl₂ to CH₂Cl₂–MeOH (9:1), gave the *title compound* (0.39 g, 69%) as an orange solid, mp 237.5–239.1 °C (Found [ES]: MH⁺, 266.0923. C₁₅H₁₂N₃O₂ [MH] requires 266.0924); IR (neat) ν_{max}/cm^{-1} 3070 (C-H), 2921 (C-H), 1596 (C-C), 1534 (NO₂), 1327 (NO₂); ¹H-NMR (500 MHz, CDCl₃) δ_H/ppm 9.30 (1H, d, *J* 1, 2'-CH), 8.82 (1H, d, *J* 2, 5-CH), 8.50 (2H, 4'-CH and 7-CH), 8.43 (1H, d, *J* 9, 4-CH), 8.28 (1H, d, *J* 9, 8-CH), 8.05 (1H, d, *J* 9, 3-CH), 7.36 (1H, d, *J* 8, 5'-CH), 2.68 (3H, s, Me); ¹³C-NMR (126 MHz, CDCl₃) δ_C/ppm 160.6 (C), 158.2 (C), 150.4 (C), 148.4 (2'-CH), 145.5 (C), 138.7 (4-CH), 135.4 (4'-CH), 131.4 (8-CH), 131.3 (C), 126.0 (C), 124.3 (5-CH), 123.4 (7-CH), 123.4 (5'-CH), 120.0 (3-CH), 24.5 (Me).

3.3.4. 2-(Pyridin-3-yl)-6-nitroquinoline (**9b**)

Biaryl **9b** was prepared according to the general procedure 3.2.1 using 2-chloro-6-nitroquinoline (**11**) (0.15 g, 0.71 mmol), 3-pyridinylboronic acid (**10b**) (0.10 g, 1.14 mmol), aqueous Na₂CO₃ (1.4 M, 1 mL) and PdCl₂(PPh₃)₂ (0.05 g, 0.07 mmol) in MeCN (3.6 mL). Purification by column chromatography on SiO₂ gel, eluting with EtOAc–CH₂Cl₂ (3:7), gave the *title compound* (0.11 g, 62%) as a yellow solid (Found [ES]: MH⁺, 252.0776. C₁₄H₁₀N₃O₂ [MH] requires 252.0767); IR (neat) ν_{max}/cm^{-1} 3081 (C-H), 1607 (C=C), 1528 (NO₂), 1337 (NO₂); ¹H-NMR (500 MHz, CDCl₃) δ_H/ppm 9.43 (1H, br s, 2'-CH), 8.84 (1H, d, *J* 2, 5-CH), 8.78 (1H, d, *J* 3, 6'-CH), 8.58 (1H, d, *J* 8, 4'-CH), 8.53 (1H, dd, *J* 9, 2, 7-CH), 8.48 (1H, d, *J* 8, 4-CH), 8.31 (1H, d, *J* 9, 8-CH), 8.08 (1H, d, *J* 9, 3-CH), 7.52 (1H, m, 5'-CH); ¹³C-NMR (126 MHz, CDCl₃) δ_C/ppm 158.0 (C), 151.2 (6'-CH), 150.4 (C), 149.0 (2'-CH), 138.9 (4-CH), 135.2 (4'-CH), 131.6 (8-CH), 128.5 (C), 128.4 (C), 126.1 (C), 124.3 (5-CH), 123.8 (C), 123.5 (7-CH), 120.2 (3-CH); *m/z* (EI) 251 (M⁺, 100), 205 (35).

3.3.5. 6-Amino-5-cyanoquinoline (**15**)

6-Nitroquinoline (0.50 g, 2.85 mmol) was added to a solution of ethyl cyanoacetate (0.91 mL, 8.61 mmol) and KOH (0.97 g, 17.0 mmol) in DMF (8.7 mL) and the mixture was stirred for 64 h. The solvent was evaporated *in vacuo* and the residue was dissolved in aqueous NaOH solution (5%; 12 mL) and heated at reflux for 3 h. The reaction mixture was allowed to cool and extracted with CHCl₃ (3 × 15 mL). The organic extracts were combined, dried (MgSO₄) and evaporated *in vacuo*. Purification by flash column chromatography on SiO₂ gel, gradient eluting with CH₂Cl₂ to CH₂Cl₂–MeOH (9:1), gave the *title compound* (0.35 g, 72%) as an orange solid, mp 181.2–182.8 °C (lit. [57] mp 181 °C) (Found [ES]: MH⁺, 170.0711. C₁₀H₈N₃ [MH] requires 170.0713); IR (neat) ν_{max}/cm^{-1} 3391 (N-H), 3337 (N-H), 3159 (C-H), 2199 (C≡N), 1635 (N-H), 1615 (C=C), 1337 (C-N); ¹H-NMR (500 MHz, CDCl₃) δ_H/ppm 8.74 (1H, d, *J* 3, 2-CH), 8.24 (1H, d, *J* 8, 4-CH), 8.06 (1H, d, *J* 9, 8-CH), 7.47 (1H, m, 3-CH), 7.15 (1H, d, *J* 9, 7-CH), 4.93 (2H, br s, NH₂); ¹³C-NMR (126 MHz, CDCl₃) δ_C/ppm 150.3 (6-C), 147.7 (2-CH), 142.4 (C), 136.0 (8-CH), 131.2 (4-CH), 128.9 (C), 123.4 (3-CH), 120.2 (7-CH), 116.1 (CN), 86.9 (5-C).

3.3.6. 3-Amino-1-(3-bromophenyl)-1H-pyrazole (**21**)

A solution of 3-bromophenyl hydrazine hydrochloride (1.36 g, 6.00 mmol), 3-methoxyacrylonitrile (1.0 mL, 12.0 mmol) and NaOEt (1.77 g, 26.0 mmol) in dry EtOH (30 mL) was heated at reflux for 20 h. After cooling the mixture to room temperature, water was added and the resultant precipitate was filtered, washed with water and finally dissolved in CH₂Cl₂. The organic extract was washed successively with water and brine, dried (MgSO₄) and evaporated *in vacuo* to give the *title compound* (1.29 g, 90%) as a yellow solid, with identical physical and spectroscopic properties to literature data [54].

3.3.7. 3-Amino-1-[3-(1H-indol-6-yl)phenyl]-1H-pyrazole (**23**)

A mixture of 3-amino-1-(3-bromophenyl)-1H-pyrazole (**21**) (0.20 g, 0.84 mmol), 6-indolylboronic acid (**22**) (0.13 g, 0.25 mmol), caesium carbonate (0.55 g, 1.68 mmol) and Pd(PPh₃)₄ (0.10 g, 0.08 mmol) in DMF (4 mL) was irradiated at 150 °C for 2 h in a sealed pressure-rated glass tube (10 mL) using

a CEM Discover microwave synthesizer by moderating the initial power (150 W). The mixture was cooled by passing a stream of compressed air through the microwave cavity and water was added (10 mL). The aqueous layer was extracted with EtOAc (3 × 20 mL) and the organic extracts were combined, washed with brine, dried (MgSO₄) and evaporated *in vacuo*. Purification by column chromatography on silica gel, eluting with hexane–EtOAc (1:1 *v/v*) gave the *title compound* [53] (0.19 g, 84%) as a colorless solid, mp 97–99 °C (Found: M⁺, 274.1218. C₁₇H₁₄N₂ [M] requires 274.1222); IR (KBr) ν_{max}/cm^{-1} 3411 (NH), 2922 (CH), 1626, 1604, 1586, 1479; ¹H-NMR (400 MHz; *d*₆-DMSO) δ_H/ppm 11.18 (1H, s, *exch.* D₂O, NH), 8.26 (1H, d, *J* 2.6, H-5), 7.96 (1H, m, H-2'), 7.69 (1H, m, H-7''), 7.63 (1H, d, *J* 8.3, H-6'), 7.58 (1H, m, H-5'), 7.46–7.41 (3H, H-4', H-2'' and H-4''), 7.35 (1H, dd, *J* 8.3, 1.6, H-4''), 6.47 (1H, m, H-3''), 5.76 (1H, d, *J* 2.6, H-4), 5.17 (2H, s, *exch.* D₂O, NH₂); ¹³C-NMR (100 MHz, *d*₆-DMSO) δ_C/ppm 157.5 (C), 134.3 (C), 141.0 (C), 137.0 (C), 133.5 (C), 130.2 (C), 128.5 (CH), 127.9 (CH), 126.8 (CH), 122.7 (CH), 120.9 (CH), 118.8 (CH), 115.2 (CH), 114.9 (CH), 110.0 (CH), 101.5 (CH), 96.7 (CH); *m/z* (EI) 275 (MH⁺, 100%), 274 (M⁺, 100), 273 (19), 246 (7), 205 (6), 191 (9), 133 (14), 84 (21).

3.3.8. 3-Amino-4-bromo-1-(3-bromophenyl)-1*H*-pyrazole (**25**)

A solution of 3-amino-1-(3-bromophenyl)-1*H*-pyrazole (**21**) (0.16 g, 0.68 mmol) and NBS (0.120 g, 0.68 mmol) in THF (10 mL) was stirred at room temperature for 16 h and then the solvent was vaporated *in vacuo*. The residue was dissolved in EtOAc, filtered through Celite and evaporated *in vacuo*. Purification by column chromatography on silica gel, eluting with hexane–EtOAc (3:1 *v/v*), gave the *title compound* (0.18 g, 83%) as a brown solid, mp 93–95 °C (Found: M⁺, 314.9005. C₉H₇⁷⁹Br₂N₃ [M] requires 314.9007); IR (KBr) ν_{max}/cm^{-1} 3415, 3312, 3213, 1629, 1594, 1556; ¹H-NMR (400 MHz; *d*₆-DMSO) δ_H/ppm 8.55 (1H, s, H-5), 7.88 (1H, m, H-2'), 7.67 (1H, m, H-5'), 7.37–7.35 (2H, m, H-4' and H-6'), 5.38 (2H, s, *exch.* D₂O, NH₂); ¹³C-NMR (100 MHz, *d*₆-DMSO) δ_C/ppm 159.9 (C), 142.5 (C), 131.8 (CH), 128.6 (CH), 127.5 (CH), 122.7 (C), 119.3 (CH), 115.1 (CH), 85.2 (C); *m/z* (EI) 275 (MH⁺, 100%); 319 (C₉H₇⁸¹Br₂N₃⁺, 61) 317 (C₉H₇⁸¹Br⁷⁹BrN₃⁺, 30), 315 (C₉H₇⁷⁹Br₂N₃⁺, 17), 220 (42), 205 (100), 189 (8), 177 (14), 145 (15), 105 (12).

3.3.9. 3-Amino-1-(4-methoxyphenyl)-1*H*-pyrazole (**28**)

The *title compound* was prepared as a yellow solid, exactly in accordance with our previously published microwave-assisted procedure [54].

3.3.10. 3-Amino-4-bromo-1-(4-methoxyphenyl)-1*H*-pyrazole (**29**)

A solution of 3-amino-1-(4-methoxyphenyl)-1*H*-pyrazole (**28**) (0.13 g, 0.68 mmol) and NBS (0.12 g, 0.68 mmol) in THF (4 mL) was irradiated at 150 °C for 2 h in a sealed pressure-rated glass tube (10 mL) using a CEM Discover microwave synthesizer by moderating the initial power (150 W). The mixture was cooled by passing a stream of compressed air through the microwave cavity and evaporated *in vacuo*. The residue was dissolved in EtOAc, filtered through Celite and the solvent was evaporated *in vacuo*. Purification by column chromatography on silica gel, eluting with hexane–EtOAc (3:1 *v/v*), gave the *title compound* (0.14 g, 77%) as a brown solid, mp 93–96 °C (Found: M⁺,

267.0015. $C_{10}H_{10}^{79}BrN_3O$ [M] requires 267.0007) IR (KBr) ν_{max}/cm^{-1} 3353 (NH), 1548, 1516, 1403, 1245, 1084, 1041; 1H -NMR (400 MHz; d_6 -DMSO) δ_H/ppm 8.34 (1H, s, H-5), 7.57 (2H, d, J 9.0, H-2' and H-6'), 6.98 (2H, d, J 9.0, H-3' and H-5'), 5.15 (2H, s, exch. D_2O , NH_2), 3.76 (3H, s, OMe); ^{13}C -NMR (100 MHz, d_6 -DMSO) δ_C/ppm 157.0 (C), 155.5 (C), 134.2 (C), 127.8 (CH), 118.5 (CH), 114.9 (CH), 95.3 (C), 55.8 (Me); m/z (EI) 269 ($C_{10}H_{10}^{81}BrN_3O^+$, 97), 267 ($C_{10}H_{10}^{79}BrN_3O^+$, 100).

3.3.11. 3-Amino-4-(4-aminocarbonylphenyl)-1-(4-methoxyphenyl)-1H-pyrazole (26)

A mixture of 3-amino-4-bromo-1-(4-methoxyphenyl)-1H-pyrazole (**29**) (0.15 g, 0.55 mmol), 4-carbamoylphenylboronic acid (**30**) (90 mg, 0.54 mmol), K_2CO_3 (0.20 g, 1.44 mmol) and $PdCl_2(PPh_3)_2$ (40 mg, 0.05 mmol) in $iPrOH-H_2O$ (1:1 v/v) (5 mL) was irradiated at 150 °C for 2 h in a sealed pressure-rated glass tube (10 mL) using a CEM Discover microwave synthesizer by moderating the initial power (150 W). The mixture was cooled by passing a stream of compressed air through the microwave cavity and water was added (10 mL). The aqueous layer was extracted with EtOAc (2 × 20 mL) and the organic extracts were combined, washed with brine, dried ($MgSO_4$) and evaporated *in vacuo*. Purification by column chromatography on silica gel, eluting with hexane–EtOAc (1:3 v/v), gave the *title compound* (90 mg, 54%) as a cream solid, mp 251–253 °C (Found: M^+ , 308.1281. $C_{17}H_{16}N_4O_2$ [M] requires 308.1273); IR (KBr) ν_{max}/cm^{-1} 3389 (NH), 1653 (C=O), 1554, 1522, 1399, 1106; 1H -NMR (400 MHz; d_6 -DMSO) δ_H/ppm 8.59 (1H, s, H-5), 7.96 (1H, br s, exch. D_2O , NHH), 7.90 (2H, d, J 8.4, H-2' and H-6'), 7.69 (2H, d, J 7.6, H-3'' and H-5''), 7.67 (2H, d, J 7.6, H-2'' and H-6''), 7.31 (1H, br s, exch. D_2O , NHH), 7.02 (2H, d, J 8.4, H-3' and H-5'), 5.18 (2H, s, exch. D_2O , NH_2), 3.51 (3H, s, OMe); ^{13}C -NMR (100 MHz, d_6 -DMSO) δ_C/ppm 168.2 (C), 158.3 (C), 155.5 (C), 135.1 (C), 133.6 (C), 132.1 (C), 128.9 (CH), 126.5 (CH), 125.5 (CH), 119.5 (CH), 116.7 (CH), 56.0 (Me); m/z (EI) 308 (M^+ , 100).

3.4. Biological Procedures

Werner syndrome fibroblast strains AG03141F, AG05229C and AG05229D were obtained from the Coriell Cell Repository (Camden, NJ, USA). All cells were cultured and treated with p38 and MK2 inhibitors and grown to replicative senescence as described previously [45]. The replicative lifespan for inhibitor treated cells is measured as a percentage of the experimental lifespan seen in the respective control (non-inhibitor treated) cells for each cell strain. The results are plotted as mean ± standard deviation. The assay to detect F-actin stress fibres and cellular morphological changes using phalloidin-FITC is exactly as described previously [45].

4. Conclusions

Suzuki-Miyaura cross-coupling reactions have been investigated for the synthesis of three different MK2 inhibitors for study in WS cells. Towards the synthesis of PF-3644022, cross-coupling of a 2-chloroquinoline with a 3-pyridinylboronic acid provided the desired biaryl target but the pyridine moiety and the chloroquinoline precursor both proved incompatible with the subsequent Yamazaki cyanation of a 6-nitroquinoline, en route to the benzothiophene ring. Thus, although a relatively early-stage Suzuki-Miyaura coupling would appear incompatible with this cyanation method,

alternative strategies for the incorporation of the 3-aminobenzo[*b*]thiophene moiety could be envisaged and thus incorporated with this transformation [58]. Towards the synthesis of a 3-aminopyrazole MK2 inhibitor, bearing a 1-[(6-indolyl)phenyl] substituent, the Suzuki-Miyaura cross-coupling reaction established one biaryl linkage, but the unprotected indole group interfered with the subsequent NBS bromination required to set up the second Suzuki-Miyaura coupling. Use of a simpler 3-aminopyrazole circumvented this problem and provided an MK2 inhibitor for study in WS cells. In all cases with simple aryl bromides, the Suzuki-Miyaura cross-coupling reactions were reliable and relatively efficient. The synthesis of the 3-amino-1-(4-methoxyphenyl)pyrazole MK2 inhibitor proceeded in three steps and 35% overall yield from commercially-available materials, each step complete in 2 h under microwave irradiation. This constitutes an extremely rapid method for access to this chemical tool, of value in elucidating the role of MK2 in accelerated aging in this progeroid syndrome. Although MK2 inhibitors may not be as useful therapeutically as p38 inhibitors, if the accelerated cell aging seen in WS does underlie the accelerated whole body aging, they may prove useful in the alleviation of the associated inflammatory conditions that are thought to be MK2 dependent and have certainly helped to suggest a role for p38-activated MK2 in replicative senescence in WS fibroblasts.

Acknowledgments

We thank the EPSRC-BBSRC-MRC sponsored network SMS-Drug (EP/I037229/1; award to MCB), Saudi Cultural Bureau (support for MB), BBSRC (BB/D524140/1; award to DK, MCB and TD), SPARC (awards to MCB and TD), ESRC under the New Dynamics of Ageing Initiative (RES-356-25-0024; award to MCB, DK and TD), EPSRC (studentship award to JD) and the R M Phillips Trust (award to MCB) for support of this work and the EPSRC Mass Spectrometry Service at the University of Wales, Swansea UK for high-resolution mass spectra.

Author Contributions

MCB participated in study design and coordination, synthesis of MK2 inhibitors, manuscript preparation and helped conceive the study, TD participated in study design, manuscript preparation, growth experiments and phalloidin assays, and helped conceive the study, DK conceived the study, participated in its design and coordination and helped to draft the manuscript, MB and IC participated in the synthesis of MK2 inhibitors and JED participated in the synthesis of MK2 inhibitors and manuscript preparation. All authors read and approved the final manuscript.

Conflicts of Interest

The authors declare no conflict of interest.

References

1. Martin, G.M.; Oshima, J.; Gray, M.D.; Poot, M. What geriatricians should know about the werner syndrome. *J. Am. Geriatr. Soc.* **1999**, *47*, 1136–1144.
2. Kipling, D.; Davis, T.; Ostler, E.L.; Faragher, R.G. What can progeroid syndromes tell us about human aging? *Science* **2004**, *305*, 1426–1431.

3. Werner, O. On Cataract Associated in Conjunction with Scleroderma. Ph.D. Thesis, Kiel University, Schmidt and Klaunig, Kiel, Germany, 1904.
4. Thannhauser, S.J. Werner's syndrome (progeria of the adult) and rothmund's syndrome: Two types of closely related heredofamilial atrophic dermatosis with juvenile cataracts and endocrine features. A critical study of five new cases. *Ann. Int. Med.* **1945**, *23*, 559–625.
5. Davis, T.; Kipling, D. Werner syndrome as an example of inflamm-aging: Possible therapeutic opportunities for a progeroid syndrome? *Rejuvenation Res.* **2006**, *9*, 402–407.
6. Yokote, K.; Hara, K.; Mori, S.; Kadowaki, T.; Saito, Y.; Goto, M. Dysadipocytokinemia in werner syndrome and its recovery by treatment with pioglitazone. *Diabetes Care* **2004**, *27*, 2562–2563.
7. Franceschi, C.; Bonafè, M.; Valensin, S.; Olivieri, F.; De Luca, M.; Ottaviani, E.; de Benedictis, G. Inflamm-aging. An evolutionary perspective on immunosenescence. *Ann. N. Y. Acad. Sci.* **2000**, *908*, 244–254.
8. Vasto, S.; Candore, G.; Balistreri, C.R.; Caruso, M.; Colonna-Romano, G.; Grimaldi, M.P.; Listi, F.; Nuzzo, D.; Lio, D.; Caruso, C. Inflammatory networks in ageing, age-related diseases and longevity. *Mech. Ageing Dev.* **2007**, *128*, 83–91.
9. Rodriguez-Lopez, A.M.; Jackson, D.A.; Iborra, F.; Cox, L.S. Asymmetry of DNA replication fork progression in Werner's syndrome. *Aging Cell* **2002**, *1*, 30–39.
10. Meyn, M.S. Chromosome instability syndromes: Lessons for carcinogenesis. *Curr. Top. Microbiol. Immunol.* **1997**, *221*, 71–148.
11. Pagano, G.; Zatterale, A.; Degan, P.; d'Ischia, M.; Kelly, F.J.; Pallardo, F.V.; Kodama, S. Multiple involvement of oxidative stress in werner syndrome phenotype. *Biogerontology* **2005**, *6*, 233–243.
12. Davis, T.; Baird, D.M.; Haughton, M.F.; Jones, C.J.; Kipling, D. Prevention of accelerated cell aging in werner syndrome using a p38 mitogen-activated protein kinase inhibitor. *J. Gerontol. A Biol. Sci. Med. Sci.* **2005**, *60*, 1386–1393.
13. Huot, J.; Houle, F.; Marceau, F.; Landry, J. Oxidative stress-induced actin reorganization mediated by the p38 mitogen-activated protein kinase/heat shock protein 27 pathway in vascular endothelial cells. *Circ. Res.* **1997**, *80*, 383–392.
14. Kim, G.Y.; Mercer, S.E.; Ewton, D.Z.; Yan, Z.; Jin, K.; Friedman, E. The stress-activated protein kinases p38 alpha and JNK1 stabilize p21(cip1) by phosphorylation. *J. Biol. Chem.* **2002**, *277*, 29792–29802.
15. Wang, W.; Chen, J.X.; Liao, R.; Deng, Q.; Zhou, J.J.; Huang, S.; Sun, P. Sequential activation of the MEK-extracellular signal-regulated kinase and MKK3/6-p38 mitogen-activated protein kinase pathways mediates oncogenic ras-induced premature senescence. *Mol. Cell. Biol.* **2002**, *22*, 3389–3403.
16. Bagley, M.C.; Davis, T.; Murziani, P.G.S.; Widdowson, C.S.; Kipling, D. Use of p38 MAPK inhibitors for the treatment of werner syndrome. *Pharmaceuticals* **2010**, *3*, 1842–1872.
17. Davis, T.; Haughton, M.F.; Jones, C.J.; Kipling, D. Prevention of accelerated cell aging in the werner syndrome. *Ann. N. Y. Acad. Sci.* **2006**, *1067*, 243–247.
18. Davis, T.; Bachler, M.A.; Wyllie, F.S.; Bagley, M.C.; Kipling, D. Evaluating the role of p38 map kinase in growth of werner syndrome fibroblasts. *Ann. N. Y. Acad. Sci.* **2010**, *1197*, 45–48.

19. Bagley, M.C.; Davis, T.; Dix, M.C.; Rokicki, M.J.; Kipling, D. Rapid synthesis of VX-745: p38 map kinase inhibition in werner syndrome cells. *Bioorg. Med. Chem. Lett.* **2007**, *17*, 5107–5110.
20. Bagley, M.C.; Davis, T.; Dix, M.C.; Fusillo, V.; Pigeaux, M.; Rokicki, M.J.; Kipling, D. Microwave-assisted ullmann C-S bond formation: Synthesis of the p38alpha MAPK clinical candidate VX-745. *J. Org. Chem.* **2009**, *74*, 8336–8342.
21. Bagley, M.C.; Davis, T.; Dix, M.C.; Fusillo, V.; Pigeaux, M.; Rokicki, M.J.; Kipling, D. Gramme-scale synthesis of the p38 α MAPK inhibitor VX-745 for pre-clinical studies into werner syndrome. *Future Med. Chem.* **2010**, *2*, 1417–1427.
22. Bagley, M.C.; Davis, T.; Dix, M.C.; Murziani, P.G.; Rokicki, M.J.; Kipling, D. Microwave-assisted synthesis of 5-aminopyrazol-4-yl ketones and the p38(MAPK) inhibitor RO3201195 for study in werner syndrome cells. *Bioorg. Med. Chem. Lett.* **2008**, *18*, 3745–3748.
23. Bagley, M.C.; Davis, T.; Dix, M.C.; Murziani, P.G.; Rokicki, M.J.; Kipling, D. Microwave-assisted synthesis of a pyrazolyl ketone library for evaluation as p38 MAPK inhibitors in werner syndrome cells. *Future Med. Chem.* **2010**, *2*, 203–213.
24. Bagley, M.C.; Davis, T.; Rokicki, M.J.; Widdowson, C.S.; kipling, D. Synthesis of the highly selective p38 MAPK inhibitor UR-13756 for possible therapeutic use in werner syndrome. *Future Med. Chem.* **2010**, *2*, 193–201.
25. Bagley, M.C.; Davis, T.; Dix, M.C.; Widdowson, C.S.; Kipling, D. Microwave-assisted synthesis of N-pyrazole ureas and the p38alpha inhibitor BIRB 796 for study into accelerated cell ageing. *Org. Biomol. Chem.* **2006**, *4*, 4158–4164.
26. Davis, T.; Wyllie, F.S.; Rokicki, M.J.; Bagley, M.C.; Kipling, D. The role of cellular senescence in werner syndrome: Toward therapeutic intervention in human premature aging. *Ann. N. Y. Acad. Sci.* **2007**, *1100*, 455–469.
27. Genovese, M.C. Inhibition of p38: Has the fat lady sung? *Arthritis Rheum.* **2009**, *60*, 317–320.
28. Bagley, M.C.; Baashen, M.; Dwyer, J.; Milbeo, P.; Kipling, D.; Davis, T. Microwave-assisted synthesis of inhibitors of MK2 for targeting p38 map kinase signalling in werner syndrome cells. In *Microwaves in Drug Discovery and Development: Recent Advances*; Spencer, J., Bagley, M., Eds.; Future Sci Ltd.: London, UK, 2014; pp. 86–104.
29. Dean, J.L.; Sully, G.; Clark, A.R.; Saklatvala, J. The involvement of AU-rich element-binding proteins in p38 mitogen-activated protein kinase pathway-mediated mrna stabilisation. *Cell Signal.* **2004**, *16*, 1113–1121.
30. Manke, I.A.; Nguyen, A.; Lim, D.; Stewart, M.Q.; Elia, A.E.; Yaffe, M.B. Mapkap kinase-2 is a cell cycle checkpoint kinase that regulates the G2/M transition and S phase progression in response to UV irradiation. *Mol. Cell* **2005**, *17*, 37–48.
31. Hegen, M.; Gaestel, M.; Nickerson-Nutter, C.L.; Lin, L.L.; Telliez, J.B. MAPKAP kinase 2-deficient mice are resistant to collagen-induced arthritis. *J. Immunol.* **2006**, *177*, 1913–1917.
32. Ronkina, N.; Kotlyarov, A.; Gaestel, M. MK2 and MK3—A pair of isoenzymes? *Front. Biosci.* **2008**, *13*, 5511–5521.
33. Duraisamy, S.; Bajpai, M.; Bughani, U.; Dastidar, S.G.; Ray, A.; Chopra, P. MK2: A novel molecular target for anti-inflammatory therapy. *Expert Opin. Ther. Targets* **2008**, *12*, 921–936.
34. Schlapbach, A.; Huppertz, C. Low-molecular-weight MK2 inhibitors: A tough nut to crack! *Future Med. Chem.* **2009**, *1*, 1243–1257.

35. Anderson, D.R.; Meyers, M.J.; Vernier, W.F.; Mahoney, M.W.; Kurumbail, R.G.; Caspers, N.; Poda, G.I.; Schindler, J.F.; Reitz, D.B.; Mourey, R.J. Pyrrolopyridine inhibitors of mitogen-activated protein kinase-activated protein kinase 2 (MK-2). *J. Med. Chem.* **2007**, *50*, 2647–2654.
36. Goldberg, D.R.; Choi, Y.; Cogan, D.; Corson, M.; DeLeon, R.; Gao, A.; Gruenbaum, L.; Hao, M.H.; Joseph, D.; Kashem, M.A.; *et al.* Pyrazinoindolone inhibitors of MAPKAP-K2. *Bioorg. Med. Chem. Lett.* **2008**, *18*, 938–941.
37. Mourey, R.J.; Burnette, B.L.; Brustkern, S.J.; Daniels, J.S.; Hirsch, J.L.; Hood, W.F.; Meyers, M.J.; Mnich, S.J.; Pierce, B.S.; Saabye, M.J.; *et al.* A benzothiophene inhibitor of mitogen-activated protein kinase-activated protein kinase 2 inhibits tumor necrosis factor alpha production and has oral anti-inflammatory efficacy in acute and chronic models of inflammation. *J. Pharmacol. Exp. Ther.* **2010**, *333*, 797–807.
38. Xiao, D.; Palani, A.; Huang, X.; Sofolarides, M.; Zhou, W.; Chen, X.; Aslanian, R.; Guo, Z.; Fossetta, J.; Tian, F.; *et al.* Conformation constraint of anilides enabling the discovery of tricyclic lactams as potent MK2 non-ATP competitive inhibitors. *Bioorg. Med. Chem. Lett.* **2013**, *23*, 3262–3266.
39. Daniels, J.S.; Lai, Y.; South, S.; Chiang, P.C.; Walker, D.; Feng, B.; Mireles, R.; Whiteley, L.O.; McKenzie, J.W.; Stevens, J.; *et al.* Inhibition of hepatobiliary transporters by a novel kinase inhibitor contributes to hepatotoxicity in beagle dogs. *Drug Metab. Lett.* **2013**, *7*, 15–22.
40. Miyaura, N.; Lahiri, K.; Suzuki, A. A new stereospecific cross-coupling by the palladium catalyzed reaction of 1-alkenylboranes with 1-alkenyl or 1-alkynyl halides. *Tetrahedron Lett.* **1979**, *36*, 3437–3440.
41. Kotha, S.; Lahiri, K.; Kashinath, D. Recent applications of the suzuki-miyaura cross-coupling reaction in organic synthesis. *Tetrahedron* **2002**, *58*, 9633–9695.
42. Suzuki, A. Recent advances in the cross-coupling reactions of organoboron derivatives with organic electrophiles 1995–1998. *J. Organomet. Chem.* **1999**, *576*, 147–168.
43. Roughley, S.D.; Jordan, A.M. The medicinal chemist's toolbox: An analysis of reactions used in the pursuit of drug candidates. *J. Med. Chem.* **2011**, *54*, 3451–3479.
44. Mavandadi, F.; Pilotti, Å. The impact of microwave-assisted organic synthesis in drug discovery. *Drug Discov. Today* **2006**, *11*, 165–174.
45. Davis, T.; Rokicki, M.J.; Bagley, M.C.; Kipling, D. The effect of small-molecule inhibition of MAPKAPK2 on cell ageing phenotypes of fibroblasts from human werner syndrome. *Chem. Cent. J.* **2013**, *7*, 18.
46. Davis, T.; Bagley, M.C.; Dix, M.C.; Murziani, P.G.; Rokicki, M.J.; Widdowson, C.S.; Zayed, J.M.; Bachler, M.A.; Kipling, D. Synthesis and *in vivo* activity of MK2 and MK2 substrate-selective p38 α (MAPK) inhibitors in werner syndrome cells. *Bioorg. Med. Chem. Lett.* **2007**, *17*, 6832–6835.
47. Davidson, W.; Frego, L.; Peet, G.W.; Kroe, R.R.; Labadia, M.E.; Lukas, S.M.; Snow, R.J.; Jakes, S.; Grygon, C.A.; Pargellis, C.; *et al.* Discovery and characterization of a substrate selective p38 α inhibitor. *Biochemistry* **2004**, *43*, 11658–11671.
48. Anderson, D.R.; Hegde, S.; Reinhard, E.; Gomez, L.; Vernier, W.F.; Lee, L.; Liu, S.; Sambandam, A.; Snider, P.A.; Masih, L. Aminocyanopyridine inhibitors of mitogen activated protein kinase-activated protein kinase 2 (MK-2). *Bioorg. Med. Chem. Lett.* **2005**, *15*, 1587–1590.

49. Anderson, D.R.; Meyers, M.J.; Kurumbail, R.G.; Caspers, N.; Poda, G.I.; Long, S.A.; Pierce, B.S.; Mahoney, M.W.; Mourey, R.J. Benzothiophene inhibitors of MK2. Part 1: Structure-activity relationships, assessments of selectivity and cellular potency. *Bioorg. Med. Chem. Lett.* **2009**, *19*, 4878–4881.
50. Anderson, D.R.; Meyers, M.J.; Kurumbail, R.G.; Caspers, N.; Poda, G.I.; Long, S.A.; Pierce, B.S.; Mahoney, M.W.; Mourey, R.J.; Parikh, M.D. Benzothiophene inhibitors of MK2. Part 2: Improvements in kinase selectivity and cell potency. *Bioorg. Med. Chem. Lett.* **2009**, *19*, 4882–4884.
51. Lee, B.S.; Lee, B.C.; Jun, J.-G.; Chi, D.Y. A new efficient synthesis of 6-nitroquipazine. *Heterocycles* **1998**, *48*, 2637–2641.
52. Tomioka, Y.; Ohkubo, K.; Yamazaki, M. Studies on aromatic nitro compounds V. A simple one-pot preparation of *o*-aminoarylnitriles from some aromatic nitro compounds. *Chem. Pharm. Bull.* **1985**, *33*, 1360–1366.
53. Velcicky, J.; Feifel, R.; Hawtin, S.; Heng, R.; Huppertz, C.; Koch, G.; Kroemer, M.; Moebitz, H.; Revesz, L.; Scheufler, C.; *et al.* Novel 3-aminopyrazole inhibitors of MK-2 discovered by scaffold hopping strategy. *Bioorg. Med. Chem. Lett.* **2010**, *20*, 1293–1297.
54. Bagley, M.C.; Baashen, M.; Paddock, V.L.; Kipling, D.; Davis, T. Microwave-assisted synthesis of 3- and 5-aminopyrazole, pyrazolo[3,4-d]pyrimidine, pyrazolo[3,4-b]pyridine and pyrazolo[3,4-b]quinolin-4-one scaffolds for mapk inhibition. *Tetrahedron* **2013**, *68*, 8429–8438.
55. Kyriakis, J.M.; Avruch, J. Mammalian mitogen-activated protein kinase signal transduction pathways activated by stress and inflammation. *Physiol. Rev.* **2001**, *81*, 807–869.
56. van Deursen, J.M. The role of senescent cells in ageing. *Nature* **2014**, *509*, 439–446.
57. Tomioka, Y.; Mochiike, A.; Himeno, J.; Yamazaki, M. Studies on aromatic nitro compounds. I. Reaction of 6-nitroquinoline with active methylene compounds in the presence of bases. *Chem. Pharm. Bull.* **1981**, *29*, 1286–1291.
58. Bagley, M.C.; Dwyer, J.E.; Molina, M.D.B.; Rand, A.; Rand, H.L.; Tomkinson, N.C.O. Microwave-assisted synthesis of 3-aminobenzo[*b*]thiophene scaffolds for the preparation of kinase inhibitors. *Org. Biomol. Chem.* **2015**, doi:10.1039/C5OB00819K.